

## Pcl/Peg Electrospun Fibers as Drug Carriers for the Controlled Delivery of Dipyridamole

Repanas A<sup>1</sup>,  
Wolkers WF<sup>1</sup>,  
Gryshkov O<sup>1</sup>, Müller M<sup>1</sup>  
Glasmacher B<sup>1</sup>

Institute for Multiphase Processes,  
Leibniz Universität Hannover, 30167  
Hannover, Germany

**Corresponding author:** Repanas A

✉ repanas@imp.uni-hannover.de

Dipl.-Pharm., MSc, Leibniz Universität  
Hannover, Institute for Multiphase  
Processes, Callinstrasse 36, 30167 Hannover,  
Germany

**Tel:** +49(0) 511 762 3824

**Fax:** +49(0) 511 762 3031

### Abstract

Electrospinning is a versatile and diverse technology for the production of nano- and microfibers that can be used as a drug delivery system (DDS). The aim of this study was to create fibrous scaffolds from a mixture of polycaprolactone (PCL) and polyethylene glycol (PEG) and to evaluate the suitability of the fibers as DDS. Dipyridamole (DPA), an anti-thrombotic and anti-proliferative pharmaceutical agent, was used as a model drug. Two types of PEG with different chain length were used. The structural, mechanical and physicochemical characteristics of the fibers with and without DPA, were determined, and the release kinetics of DPA were studied. The obtained fibers loaded with DPA and with the higher molecular weight PEG were smooth and had an average diameter of  $586.75 \pm 204.79$  nm and an average Young's modulus of  $57.14 \pm 4.35$  MPa, whereas the tensile strain at break was  $0.61 \pm 0.05$  mm/mm and the ultimate tensile strength (UTS) was  $16.79 \pm 3.08$  MPa. The cumulative release of DPA revealed two stages: an initial burst phenomenon followed by slower Fickian diffusion (release exponent  $n = 0.432$ ).

**Keywords:** Anti-platelet treatment; Biomaterials; Electrospinning; Polycaprolactone; Polyethylene glycol; Dipyridamole

**Abbreviations:** DPA: Dipyridamole; PCL: Polycaprolactone; PEG: Polyethylene Glycol; DDS: Drug Delivery System; TFE: 2,2,2-Trifluoroethanol; PBS: Phosphate Buffer Solution; SEM: Scanning Electron Microscopy; FTIR: Fourier Transform Infrared Spectroscopy; UTS: Ultimate Tensile Strength

### Introduction

Electrospinning is a promising technology that can be used to create fibrous scaffolds in the nanoscale range for biomedical applications [1]. The basic principle of this simple, versatile and cost-efficient technique is the application of a strong electrical field to eject a polymer solution from a reservoir to a collector producing non-woven fiber networks. Solution properties such as the concentration and molecular weight of solvents and polymers, as well as processing parameters, such as the spinning distance and the solution flow rate affect the morphological, physical and biomechanical properties of the generated fibers [2]. A typical setup of an electrospinning apparatus consists of three basic elements: a high voltage power supply, a solution reservoir and a grounded collector [3]. Due to the wide range of available materials, electrospinning technology has turned into

a powerful tool for the fabrication of micro- or nano-structures suitable for applications in the fields of tissue engineering and drug delivery [4-7]. Polycaprolactone (PCL) is a semi-crystalline, highly hydrophobic polymer that is easily soluble in most organic solvents, and has been approved by the Food and Drug Administration (FDA) in the USA for biomedical uses [8]. PCL has good miscibility properties, possesses mechanical stability and displays prolonged degradation. Moreover, it can be easily electrospun and can be used for long-term sustained delivery of pharmaceutical agents in the field of drug delivery and tissue engineering [9-13]. On the other hand, polyethylene glycol (PEG) is a water soluble polyether with a wide range of molecular weights that has been found to be biocompatible and has been used in hydrogels, for surface modification of other polymers to obtain co-polymers, control of protein adsorption and as an adhesion molecule [14]. Therefore, the use of both polymers as

a single blend could lead to products that exhibit a combination of properties, suitable for applications in drug delivery.

The ability to diffuse into the surrounding medium as well as the release kinetics of a drug that has been loaded in a polymeric carrier depend on various factors, including the solubility and the possibility of swelling of the polymeric matrix in the medium according to Tungprapa et al.[15]. Moreover, when a pharmaceutical agent is loaded inside a biodegradable polymeric carrier, two distinct major mechanisms are known to facilitate the drug release, mainly polymer degradation and small molecule diffusion [16]. PCL displays little degradation in aqueous environment during the first months [8], whereas PEG is a water soluble polymer that can be immediately dissolved in the surrounding medium. PEG also enhances the stability of biomolecules and affects release characteristics [17]. In addition, if PCL is the predominant polymer in the fabricated electrospun fibers, diffusion through the polymeric matrix is expected to be the major mechanism [18]. The aim of this work was to fabricate fibrous scaffolds from a polymeric blend of PCL and PEG with an incorporated model drug, in order to create a drug delivery system (DDS), which would enable encapsulation and sustained delivery of the pharmaceutical agent. Dipyridamole (DPA) was used as a model drug. The release kinetics from electrospun scaffolds and the effect of its presence on the properties of the fabricated fibers were studied. DPA is used as an antiplatelet agent, either alone or in combination with other pharmaceutical agents in order to reduce the risk of stroke incidents after a severe cardiovascular event, such as myocardial infarction [19,20]. Additionally, it can increase gap junction coupling in aortic endothelial and vascular smooth muscle cells [21,22]. One of the conclusions of these studies was that DPA is best utilized in sustained release forms of administration like microspheres. A DDS enabling controlled release of DPA can be used in drug delivery applications [23,24]. PEG with different molecular weight was used to investigate the influence of the polymeric chain length on the properties of the scaffolds. Electrospun PCL fibers without PEG served as control. The structural, morphological, mechanical and physicochemical properties of the electrospun scaffolds were evaluated. The cumulative *in vitro* release of DPA was monitored and analyzed throughout a period of ninety six days to investigate the release kinetics of DPA by fitting the obtained data according to the model described by Ritger and Peppas (1987) [25]. The choice of PCL as the main polymer was based on the fact that in order to create a proper DDS system for the sustained release of DPA, a slow degrading polymer (recognized as a suitable material for the fabrication of scaffolds, as it was previously discussed), which would be also inexpensive and easy to process, was needed. In addition, as it was previously mentioned, PEG was used to enhance the stability of the encapsulated pharmaceutical molecules and to augment the miscibility of the polymeric solution. Furthermore, since PEG types with various molecular weights are available, it enables to adjust the fibers' characteristics with regard to release kinetics of the encapsulated drug, via its polymeric chain length. It is also inexpensive and presents good miscibility with PCL, a feature that has been previously described [26]. Therefore, the combination of the two polymers was considered suitable to create a DDS for DPA encapsulation. In a nutshell, a DDS system based on PCL/PEG fibers can be considered as a suitable drug

carrier candidate of DPA in order to be further tested as a novel solution for an alternative anti-coagulant therapeutic strategy for patients that are at high risk of stroke, myocardial infarction, thrombotic incidents and other life threatening situations. The use of electrospinning and fiber technology for the creation of a proper DDS system for DPA has only been used once in the past for the creation of poly-urethane tubular scaffolds [23] and by our group for the creation of PCL based DDS [24]. Therefore, further research needs to be conducted in order to have a better understanding of the use of fibers for this application. However, the idea of controlling the characteristics of the fibers and DPA's release kinetics via the polymeric chain length of PEG is novel and very promising for the mentioned DDS, and it was one of the basic goals of this work. Finally, the outcome of this study can be used as an initial step to promote future research on DDSs based on PCL/PEG fibers made by electrospinning for similar pharmaceutical agents.

## Materials and Methods

### Materials

Polycaprolactone (PCL) (Mn 70000-90000) and dipyridamole (DPA) ( $\geq 98.0\%$ ) were purchased from Sigma-Aldrich. Polyethylene glycol (PEG) (Mr 3500-4500 & Mr $\sim$ 35000) was purchased from Fluka. 2,2,2-trifluoroethanol (TFE) was purchased from abcr GmbH & Co.KG. All materials and reagents were used as received without any further purification.

### Preparation of the polymeric solutions

Both the polymers and DPA were dissolved in TFE. The total polymer concentration was 150 mg/mL and the mass ratio between PCL and PEG was 3:1. The concentration of DPA in the solution was 10 wt% of the mass of PEG. The concentrations of PCL and PEG were selected based on previous preliminary experiments taking into account the ease of electrospinning of the solutions and the solubility of the materials used in TFE. For example, a 50:50 polymer ratio of PCL and PEG led to fibers with beads, wider diameter distributions and to an unstable electrospinning process (**Figure 1**). In addition, a solution with the same polymer concentration and mass ratio but without DPA was also prepared to serve as a control. Furthermore, blend solutions of PCL with and without DPA were prepared as additional control groups. In that case, the concentration of PCL was 150 mg/mL while the concentration of DPA remained the same as that of the solutions with PEG. All polymeric solutions were constantly stirred for 18h at room temperature in order to achieve homogenous mixtures.

### Electrospinning process

Disposable blunt-tipped needles (21G, Nordson EFD) with an inner diameter of 0.6 mm and 5 mL syringes (Omnifix, B. Braun) were used as the polymeric solution reservoirs. The solution flow rate was kept at 4 mL/h with an applied voltage of 25 kV in order to achieve continuous flow with no jet breaks. The distance between the tip of the needle and the grounded, square aluminum collector (15 $\times$ 15 cm<sup>2</sup>) was kept constant at 25 cm. In addition, an aluminum foil covering the surface of the collector

was used to retrieve the electrospun fiber mats. Moreover, electrospinning was performed under stable conditions of temperature and relative humidity ( $T=21 \pm 1.5$ , Rel. Humidity =  $30 \pm 5\%$ ) for 30min per sample. After the press, the samples were removed from the collector and left to dry under vacuum for 24h. The sample group with DPA and PEG (Mr 35000, PEG35k) are designated as F1 and the one without DPA as F0 for better comprehension. Furthermore, the electrospun fibers composed of PEG (Mr 4000, PEG4k) but without DPA and are designated as F2 and the ones with incorporated DPA as F3. Finally, the sample groups without DPA and only PCL are designated as F4 and the ones with incorporated DPA as F5. The concentrations of all materials and the short code names are summarized in **Table 1**.

### Characterization of the electrospun fiber mats

**Electrical conductivity:** A conductometer (SevenMulti, Mettler Toledo AG) was used to measure the electrical conductivity of the polymeric solutions. 2 mL of each solution were measured at 25. All measurements were carried out in quintuplicate.

**Scanning electron microscopy (SEM):** Square strips of  $5 \times 5$  mm<sup>2</sup> were carefully punched out from all sample groups and were sputter coated with Au/Pd for 60s before being mounted on a steel stage inside the SEM (S3400N, Hitachi), (15 kV, high vacuum). In order to determine the average fiber diameter, pictures obtained at a magnification of 4000x were pressed using the image analysis software ImageJ (National Institutes of Health), taking measurements of 75 different fibers from 5 different samples from all groups.

**Fourier transform infrared spectroscopy (FTIR):** Infrared absorption measurements were carried out with a Perkin Elmer 100 Fourier transform infrared (FTIR) spectrometer (Perkin Elmer, Norwalk, CT, USA), equipped with a triglycine sulfate (TGS) detector and an attenuated total reflection (ATR) accessory with a diamond/ZnSe crystal. The acquisition parameters were: 4 cm<sup>-1</sup> resolution, 8 co-added interferograms, and 4000 - 650 cm<sup>-1</sup> wavenumber range. Spectra analysis and display were carried out using Perkin Elmer software (Perkin Elmer, Norwalk, CT, USA).

**Mechanical tensile testing:** Rectangular strips of 15 mm gauge length and 10 mm width were carefully punched out from all groups. The thickness of each individual specimen was measured with a thickness gauge (Quick mini, Mitutoyo). Double-edged duct tape was carefully placed at both edges of the strips to facilitate their mounting on the metallic grips of the testing device. Uniaxial tensile tests were conducted with an INSTRON 5967 Dual Column tensile testing instrument with a 100 N load cell (Instron, USA). The ultimate tensile strength (UTS), the tensile strain at maximum force and the Young's modulus values were analyzed. All the experiments were conducted at room temperature. An elongation rate of 1 mm/s was applied to the samples. Six samples were tested per group.

**In vitro drug release study:** For the drug release experiments, square strips of  $10 \times 10$  mm<sup>2</sup> were punched out from the electrospun specimens, subsequently immersed in 1 mL of phosphate buffer solution (PBS) and kept in 2 mL tubes (Eppendorf) inside a waterbath at 37. At predefined time points, the total volume of the PBS medium was removed for measuring the absorbance

and fresh medium was added back to the tube. The absorbance of DPA was measured at 284 nm using a UV-Vis spectrometer (LIBRA S22, Bihrom) and plastic, disposable UV-cuvettes (1.5 mL, 12.5x12.5x45 mm, Brand). A calibration plot of absorbance versus concentration was created using standard solutions of DPA in PBS with concentrations ranging from 1 µg/mL up to 50 µg/mL. The cumulative release of DPA was measured for a total period of 96 days. All experiments were carried out in triplicates.

**Release kinetics mechanism:** The release kinetics of DPA were analyzed using the equation described by Ritger PL and Peppas NA (1987) [25].

$$M_t/M_\infty = kt^n \quad \text{Equation 1}$$

where  $M_t$  is the drug released at the time point  $t$ ,  $M_\infty$  is the total amount of drug released,  $k$  is a constant depending on the structural and geometrical characteristics of the drug carrier and  $n$  is the release exponent which indicates the release mechanism.

**Statistical analysis:** All data are expressed as mean  $\pm$  standard deviation unless otherwise mentioned. One-way analysis of variance (ANOVA) with post h Tukey means comparison tests were conducted and  $p$  value  $< 0.05$  was considered significant. The distribution of values in terms of normality was assessed before one-way ANOVA analysis in order to ensure the quality of the obtained results.

## Results

### Structural and morphological analysis

The obtained SEM pictures of the fibers are shown in **Figure 2**. SEM images of the investigated specimens revealed no drug aggregates and beads, indicating adequate miscibility of all the materials and confirming a stable and repeatable press. In all cases, electrospinning resulted in cylindrical fibers with smooth surface and diameters in the sub-micron/nano- scale forming dense networks. That was made possible by selecting the appropriate PCL/PEG ratio during preliminary results (**Figure 1**). The average fiber diameter of specimens F0, F1, F2, F3, F4 and F5 fibers were found to be  $661.33 \pm 196.94$  nm,  $586.75 \pm 204.79$  nm,  $617 \pm 208.96$  nm,  $558 \pm 190.08$  nm,  $1005.33 \pm 319.44$  nm and  $771.33 \pm 247.9$  nm, respectively. **Figure 3** captures the

**Table 1** Short code names and materials' concentrations (mg/mL) for electrospun fibers prepared using Polycaprolactone (PCL), Polyethylene glycol (PEG, two different average molecular weight types) and Dipyrindamole (DPA).

Sample name	PCL concentration mg/mL	PEG concentration mg/mL	DPA concentration mg/mL
F0	112.5	37.5 (PEG35k) <sup>a</sup>	-
F1	112.5	37.5 (PEG35k) <sup>a</sup>	3.75
F2	112.5	37.5 (PEG4k) <sup>b</sup>	-
F3	112.5	37.5 (PEG4k) <sup>b</sup>	3.75
F4	150.0	-	-
F5	150.0	-	3.75

<sup>a</sup> PEG Mr~35000, <sup>b</sup> PEG Mr 3500-4500

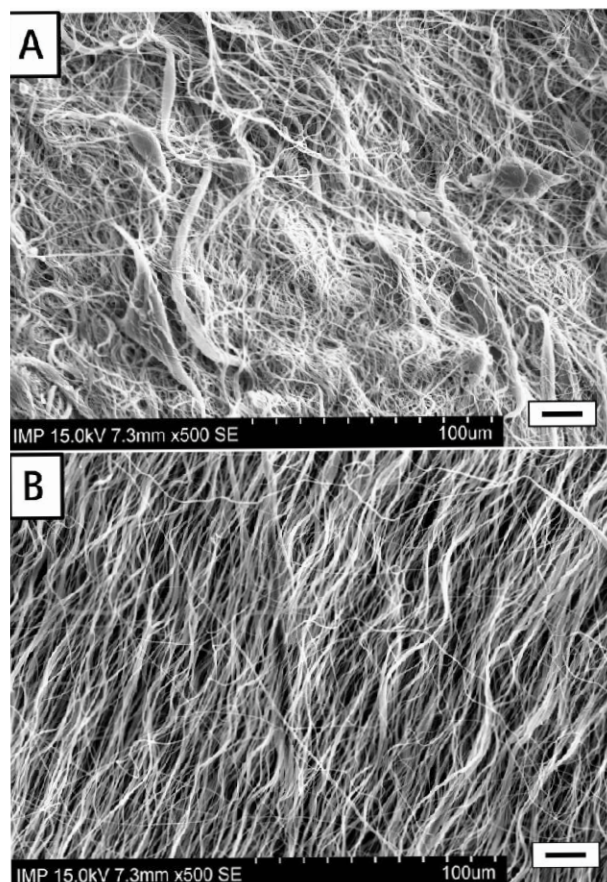


**Figure 1** SEM pictures of electrospun fibers with a 50:50 mass ratio between PCL and PEG (A) and fibers with a 75:25 mass ratio between the two polymers (B); 15 kV accelerating voltage, high vacuum, 500x magnification, scale bars = 20  $\mu\text{m}$ .

differences between all the different electrospun fiber specimens. No significant differences were observed between fibers F0 and F1, as well as between fibers F2 and F3. The average fiber diameter of specimen F5 differed significantly from fibers F1, F2, F3 ( $p < 0.001$ ). Finally, fibers F5 also differed significantly with fibers F4 ( $p < 0.05$ ). The histograms of the calculated diameters of the electrospun fibers are also depicted in **Figure 2**. The fiber diameter distribution of the specimens F0, F1, F2 and F3 were found to be similar, whereas F4 displayed a broader fiber diameter distribution. In case of specimen F5, the addition of DPA resulted in a narrower fiber diameter distribution (**Figure 2**). In addition, no particular alignment was observed (**Figure 2**).

### Physicochemical characterization

The addition of DPA to the polymeric solutions significantly affected the electrical conductivity (**Figure 4**), which increased from  $1.556 \pm 0.09 \mu\text{S}/\text{cm}$  for F0 fibers to  $6.272 \pm 0.152 \mu\text{S}/\text{cm}$  for F1 fibers; from  $1.912 \pm 0.03 \mu\text{S}/\text{cm}$  for F2 fibers to  $6.716 \pm 0.12 \mu\text{S}/\text{cm}$  for F3 fibers and from  $0.521 \pm 0.023 \mu\text{S}/\text{cm}$  for F4 fibers to  $18.81 \pm 0.058 \mu\text{S}/\text{cm}$  for F5 fibers, presenting a statistically significant difference ( $p < 0.001$ ). In order to investigate physicochemical interactions between the electrospun fibers loaded with DPA and the bulk materials, FTIR was used

as a means of chemical characterization. **Figure 5** depicts the FTIR spectra of F1 and F0 fibers compared with the ones from bulk PCL and PEG pellets as well as DPA crystalline powder. The spectrum of the PCL pellets exhibited characteristic peaks at  $2943 \text{ cm}^{-1}$  (-CH<sub>3</sub>, asymmetric stretching),  $2869 \text{ cm}^{-1}$  (-CH<sub>3</sub>, symmetric stretching) and  $1725 \text{ cm}^{-1}$  (-C=O, stretching) in agreement with previous studies [26]. Furthermore, the FTIR spectrum of bulk PEG exhibited characteristic peaks at  $2882 \text{ cm}^{-1}$  (-CH<sub>3</sub>, symmetric stretching),  $1342 \text{ cm}^{-1}$  (-CH<sub>3</sub>, scissoring and bending) and  $1095 \text{ cm}^{-1}$  (-C-O-C<sub>(ether)</sub> stretching). Moreover, the spectrum of DPA in powder form exhibited the following characteristic peaks among other: at  $2921 \text{ cm}^{-1}$  (-CH<sub>3</sub>, asymmetric stretching) and at  $1531 \text{ cm}^{-1}$  (-C=N, stretching). Additionally, F0 specimens exhibited characteristic peaks at  $2946 \text{ cm}^{-1}$  (-CH<sub>3</sub>, asymmetric stretching),  $1723 \text{ cm}^{-1}$  (-C=O, stretching),  $1342 \text{ cm}^{-1}$  (-CH<sub>3</sub>, scissoring and bending),  $1103 \text{ cm}^{-1}$  (-C-O-C<sub>(ether)</sub> stretching). On the other hand, the spectrum of the F1 fibers exhibited a mixture of characteristic peaks from the spectra of the bulk materials. More specifically, F1 fibers exhibited characteristic peaks at  $2946 \text{ cm}^{-1}$  (-CH<sub>3</sub>, asymmetric stretching),  $1726 \text{ cm}^{-1}$  (-C=O, stretching),  $1342 \text{ cm}^{-1}$  (-CH<sub>3</sub>, scissoring and bending),  $1100 \text{ cm}^{-1}$  (-C-O-C<sub>(ether)</sub> stretching) and a low absorbance peak at  $1536 \text{ cm}^{-1}$ , corresponding to -C=N stretching from DPA. The differences in peaks of the F0 and F1 specimens as well as from the bulk materials are summarized in **Table 2**.

### Mechanical characterization

The obtained data from the mechanical tensile tests are presented in **Figure 6**. The average UTS increased from  $14.32 \pm 1.51 \text{ MPa}$  for the F0 fibers to  $16.79 \pm 3.08 \text{ MPa}$  for the F1 electrospun fibers (**Figure 6A**). Moreover, F3 specimens exhibited higher UTS ( $13.94 \pm 1.87 \text{ MPa}$ ) compared to F2 specimens ( $11.32 \pm 1.93 \text{ MPa}$ ). In addition, the average UTS values of specimens F4 and F5, which were  $58.15 \pm 4.75 \text{ MPa}$  and  $60.27 \pm 6.48 \text{ MPa}$  respectively, were significantly higher than the rest of the specimens ( $p < 0.001$ ). However, the addition of DPA in specimens F1, F3 and F5 did not result in significant increase of the UTS values ( $p > 0.05$ ) (**Figure 6A**). Additionally, the tensile strain at break was  $0.62 \pm 0.06 \text{ mm}/\text{mm}$  and  $0.61 \pm 0.05 \text{ mm}/\text{mm}$  for fibers F0 and F1, respectively (**Figure 6B**), indicating that DPA has little effect on mechanical properties. A minor decrease in the tensile strain values was observed between specimens F2 and F3. More specifically, the tensile strain at break dropped from  $0.38 \pm 0.05 \text{ mm}/\text{mm}$  to  $0.30 \pm 0.02 \text{ mm}/\text{mm}$ , but not significantly ( $p > 0.05$ ). The use of PEG with different molecular weight with and without incorporated DPA led to a statistical difference in terms of tensile strain ( $p < 0.001$ ). Moreover, the specimens fabricated only by PCL (F4) exhibited the highest tensile strain at break, namely  $0.8 \pm 0.09 \text{ mm}/\text{mm}$ , and were statistically different from all the other specimens ( $p < 0.001$ ). Finally, the average tensile strain at break of fibers F5 was  $0.45 \pm 0.05 \text{ mm}/\text{mm}$ . The differences between the Young's modulus values are depicted in **Figure 6C**. The presence of DPA in specimens F1, F3 and F5 led to an increase in the average Young's modulus values from  $48.69 \pm 6.46 \text{ MPa}$  to  $57.14 \pm 4.35 \text{ MPa}$  for fibers F0 and F1; from  $65.87 \pm 6.66 \text{ MPa}$  to  $107.05 \pm 9.29 \text{ MPa}$  for fibers F2 and F3 and from  $98.9 \pm 16.35 \text{ MPa}$  to  $199.98 \pm 33.78 \text{ MPa}$  for fibers F4 and F5, respectively. Fibers F5 exhibited the highest average Young's modulus, which was statistically different from

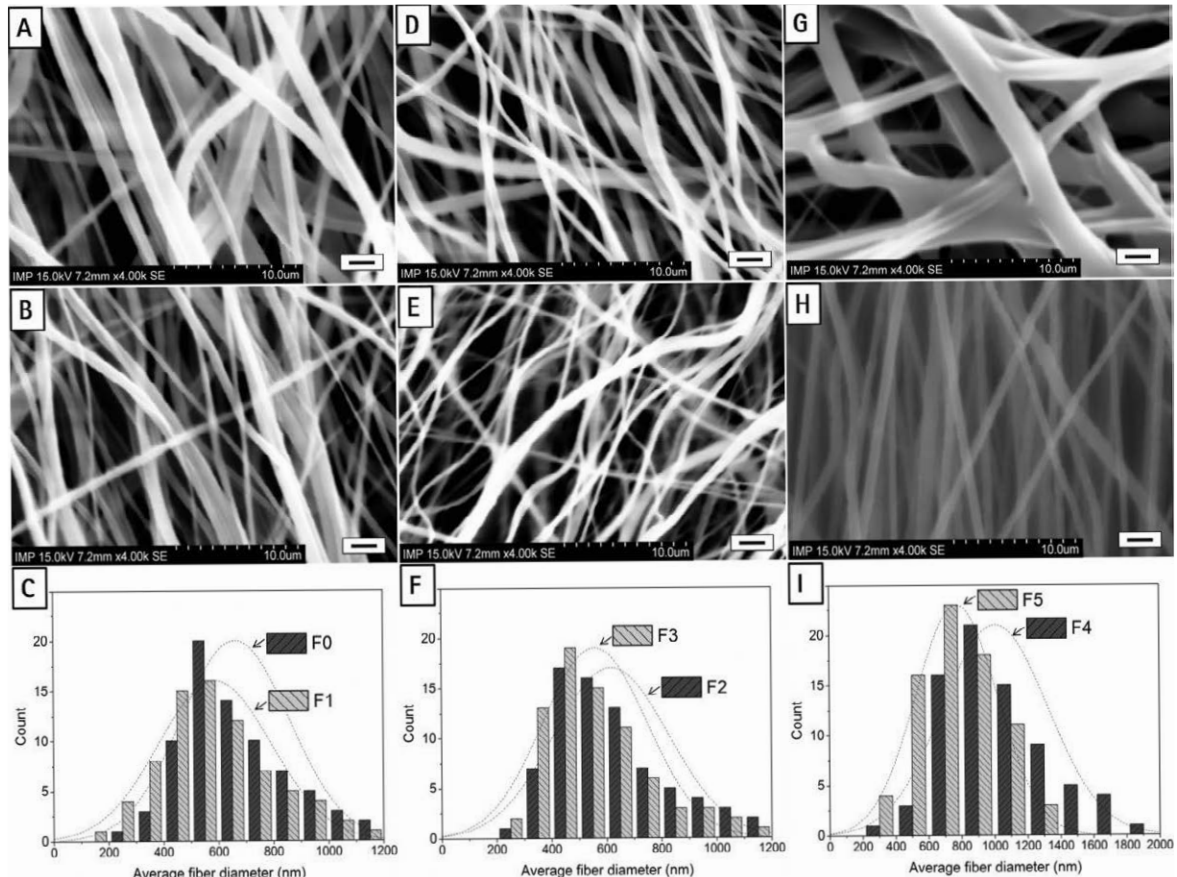


**Figure 2** SEM pictures of electrospun F0 fibers (PCL & PEG35k) with no Dipyridamole (DPA) encapsulated (A); F1 fibers (PCL & PEG35k) with DPA encapsulated (B); Histogram of the fiber diameter distributions of fibers F0 and F1 (C); F2 fibers (PCL & PEG4k) with no Dipyridamole (DPA) encapsulated (D); F3 fibers (PCL & PEG4k) with DPA encapsulated (E); Histogram of the fiber diameter distributions of fibers F2 and F3 (F); F4 fibers (PCL) with no Dipyridamole (DPA) encapsulated (G); F5 fibers (PCL) with DPA encapsulated (H); Histogram of the fiber diameter distributions of fibers F4 and F5 (I); 15 kV accelerating voltage, high vacuum, 4000x magnification, scale bars = 1  $\mu$ m.

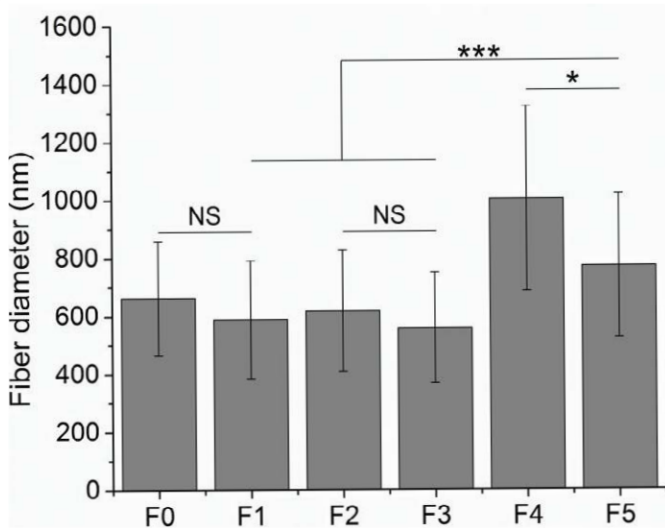


**Figure 3** Average fiber diameter values from electrospun fibers F0-F5 obtained after image analysis using ImageJ; (mean  $\pm$  SD, n = 75); One-way ANOVA with post hoc Tukey (\*  $p < 0.05$ , \*\*  $p < 0.001$ , \*\*\*  $p < 0.001$ , NS = not significant).

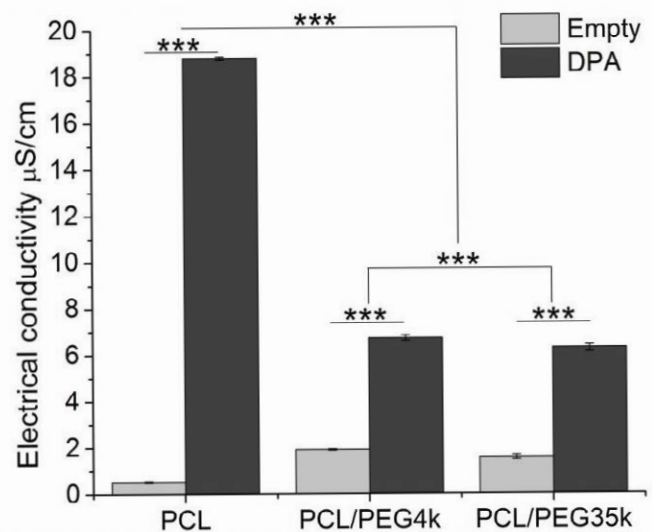


**Figure 4** Electrical conductivity values from the polymeric solutions used to fabricate electrospun specimens F0-F5, (mean  $\pm$  SD, n=5); One-way ANOVA with post hoc Tukey (\*  $p < 0.05$ , \*\*  $p < 0.001$ , \*\*\*  $p < 0.001$ , NS = not significant).

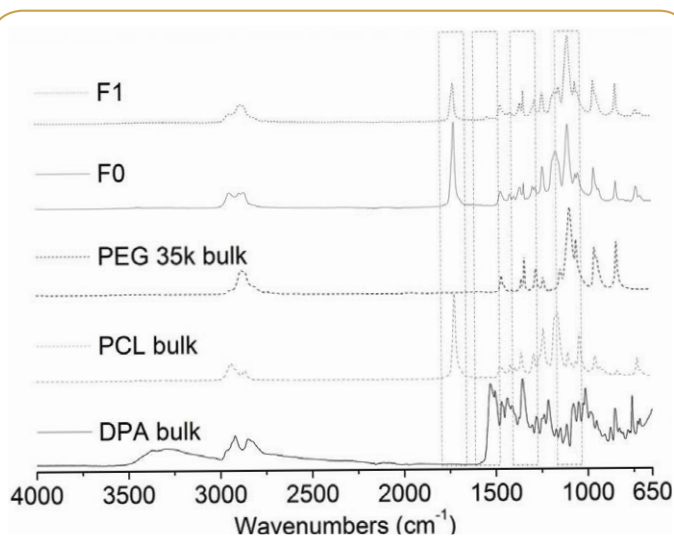


**Figure 5** FTIR spectra of PCL pellets, bulk PEG, powder DPA, F0 and F1 electrospun fibers from 4000 to 650  $\text{cm}^{-1}$ ; the dotted rectangular sites indicate the differences in the spectra between F0, F1 fibers and bulk materials.

all the other samples ( $p < 0.001$ ). In addition, Young's modulus values from fibers F2 and F3 were statistically different ( $p < 0.01$ ) while there was no significant difference between fibers F0 and F1 ( $p > 0.05$ ). Finally, the use of PEG with different molecular weight led to a significant difference in Young's modulus values between fibers F1 and F3 ( $p < 0.001$ ).

### Cumulative drug release experiments

The cumulative amount of DPA released from F1, F3 and F5 specimens was calculated as the fraction of the total DPA content inside a PBS solution (pH 7.4,  $T = 37^\circ\text{C}$ ). The drug release studies were performed in an incubator over a period of 96 days. The cumulative release profile of DPA from the electrospun fibers is shown in **Figure 7**, while the inset depicts the first day of DPA release. Two distinct release stages could be identified for all the different electrospun specimens: a rapid burst release followed by a relatively slow release phase. During the initial 24h, F1 fibers showed a burst release of DPA, where  $52.4 \pm 1.1\%$  of DPA released into the PBS medium. In comparison with this, F3 and F5 showed  $60.32 \pm 1.82\%$  and  $63.14 \pm 1.07\%$  release of DPA into the medium, respectively. The first stage where more than half of DPA mass was already released for all different electrospun specimens was followed by a successive slow second stage. During this stage the cumulative release of DPA was lower and more gradual, reaching  $84.74 \pm 1.06\%$  until the 18<sup>th</sup> day for fibers F1. In addition, the cumulative release of DPA from fibers F3 and F5 was  $93.79 \pm 2.02\%$  and  $95.89 \pm 1.43\%$ , respectively. Moreover, the release rate of DPA was gradually decelerating, ultimately reaching a plateau. The cumulative release of DPA reached  $89.07 \pm 1.29\%$  for F1 fibers,  $97.55 \pm 1.71\%$  for F3 fibers and  $98.17 \pm 1.59\%$  for F5 fibers on the 96<sup>th</sup> day.

In order to comprehend the mechanism that regulates the release of DPA, the data obtained from the cumulative release studies were fitted according using Equation 1 [27]. In **Figure 7** (inset) the release exponent  $n$  for F1, F3 and F5 fibers is depicted together with an attempt to fit the obtained experimental data.

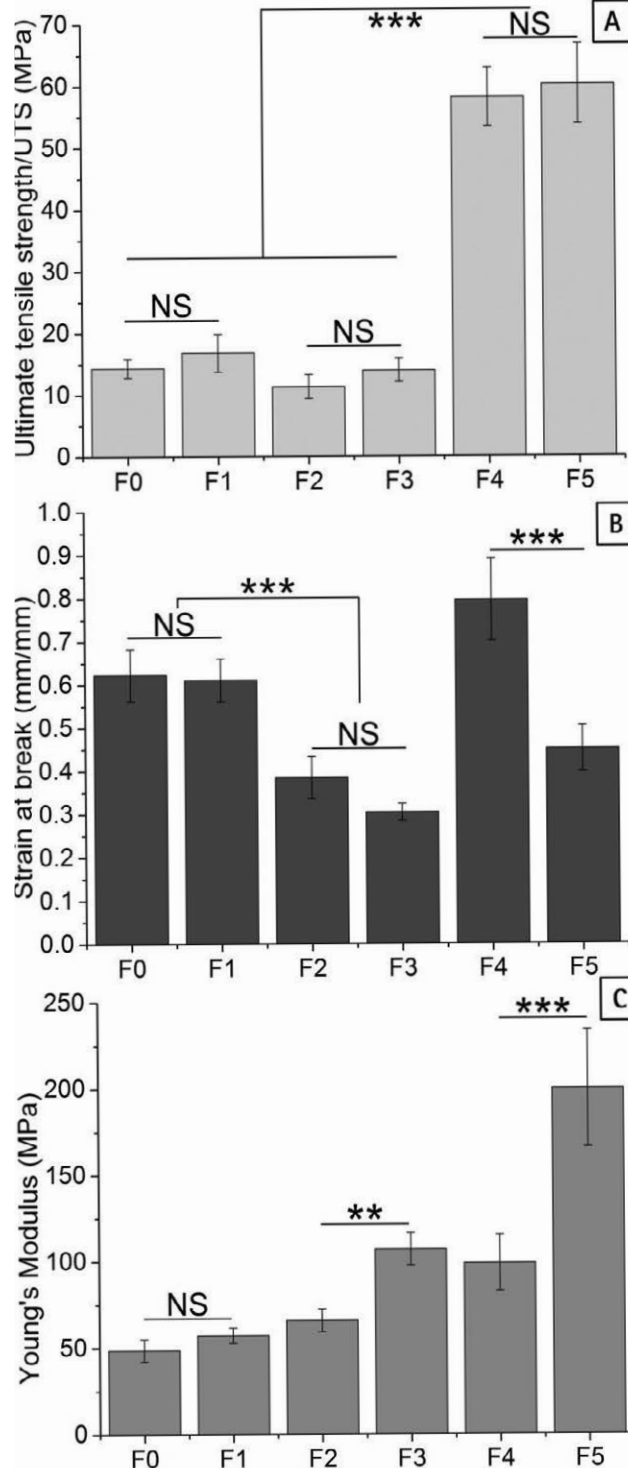


**Figure 6** Mechanical properties of the F0-F5 electrospun fibers. Ultimate tensile strength (UTS) (A); tensile strain at break (B); and Young's modulus (C); elongation rate=1mm/sec; (mean  $\pm$  SD,  $n = 6$ ); One-way ANOVA with post hoc Tukey (\*  $p < 0.05$ , \*\*  $p < 0.001$ , \*\*\*  $p < 0.001$ , NS = not significant).

The release exponents  $n$  for specimens F1, F2 and F3 were 0.432, 0.454 and 0.426 respectively, corresponding to Fickian diffusion ( $R^2 > 0.93$  for all cases).

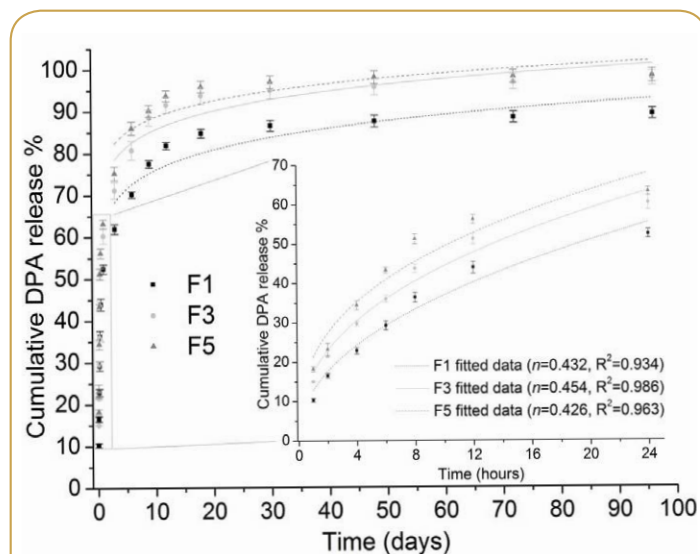


**Figure 7** Cumulative release of DPA from F1, F3 and F5 electrospun fibers during a total 96 days period; cumulative release of DPA from F1, F3 and F5 fibers during the initial 24 hours (inset); (mean  $\pm$  SD,  $n = 3$ );  $T = 37^\circ\text{C}$ ; Experimental and fitted data (using Equation 1 described by Peppas et al.,  $M_t/M_\infty = kt^n$ ) from F1, F3 and F5 fibers during the first 60% of DPA released; (mean  $\pm$  SD,  $n = 3$ ).

## Discussion

Electrospun fibers loaded with DPA and without DPA were fabricated using different molecular weight of PEG. The obtained fibers had an average diameter between 600 nm and 1000 nm (**Figure 3**). The addition of DPA in the polymeric solutions resulted in a significant increase of the solution's electrical conductivity, while at the same time decreasing the average fiber diameter. On the other hand, addition of PEG led to a significant increase in the average values of electrical conductivity and a decrease in the average fiber diameter compared to the fibers containing only PCL. Additionally, higher molecular weight of PEG resulted in polymeric solutions with lower average values of electrical conductivity and consequently to thicker fibers. Similar findings concerning the influence of molecular weight of PEG on fiber diameter and electrical conductivity were described by Saraf et al [28]. According to Lee et al., decrease in the average fiber diameter could be the result of the increase in the solutions conductivity due to augmented transfer of electrical charges into the polymeric jet [29], resulting in greater bending instability of the solution inside the electrical field. Consequently, further elongation of the jet cured, leading to thinner fibers. Furthermore, the presence of chemical groups (pH dependant) in DPA (hydroxyl groups), could have further increased the electrical conductivity [30]. FTIR spectroscopy was used to study the possible differences between the electrospun fibers and the bulk materials, as well as between the polymers and DPA (**Figure 5**). Shifts in the peaks could be indicative of different intermolecular interactions in the fibers. More specifically, there are various changes in the peaks of the F1 fibers compared with the spectra of fibers F0, bulk PCL and PEG (**Table 2**). The resulting peaks of the F1 spectrum could be an aftermath of a possible interaction between PCL and PEG. On the other hand, the peaks of DPA were very difficult to be

identified in the fibers due to the mass ratio of the materials used. Nevertheless, a low intensity peak at  $1536\text{ cm}^{-1}$  ( $-\text{C}=\text{N}$ , stretching) was detected in the F1 spectrum, which was shifted compared with the peak in the DPA spectrum, whereas no peak was observed in the spectrum of F0 fibers. Furthermore, the differences between the spectra of bulk PCL and F1 fibers could be the result of different degree of PCL crystallinity before and after it was dissolved in TFE and electrospun [31]. In addition, formation of hydrogen bonds between the ester groups of PCL (in a semi-crystalline state) and the hydroxyl groups of TFE (in an amorphous state) molecules could explain the shifts in the absorption bands [32,33]. The addition of DPA in the blend solutions increased the average values of UTS and Young's modulus where the addition of DPA resulted in stiffer fibers. The influence of DPA and PEG on the solution's electrical conductivity as well as on the average fiber diameter can also affect the mechanical properties. The decrease in the average fiber diameter and minor change in the general alignment and structure of the fibers affect mechanical properties [34]. Moreover, differences in intermolecular interactions between the polymers might explain these differences in mechanical properties. The FTIR data endorse this hypothesis since there were shifts in characteristic peaks of the fiber spectra compared with that of the bulk materials, but also between F0 and F1. The use of low molecular weight PEG with lower average polymeric chain length (F2 & F3) led to weaker and less flexible but stiffer fibers indicating that the length of the polymeric chain determines mechanical properties of the fabricated scaffolds. Moreover, the fibrous scaffold's architecture in the nano-/submicron level is considered very important for the release of the encapsulated molecule. The stresses that a scaffold would possibly confront from the surrounding environment at the site of implantation affect the structure of the carrier and thus the release kinetics [35]. Two distinct stages of DPA release were observed in all cases: a strong burst release phenomenon followed by a slower release phase. The initial burst release stage that was particularly intense during the first 12 hours (**Figure 7**, inset), has been previously described by other groups [36-38]. According to Zamani et al., it is possible that a considerable amount of the drug could have migrated to the surface of the ejected polymer solution during electrospinning [11]. Additionally, DPA might have been incorporated into the amorphous regions of the semi-crystalline PCL. Kim et al. proposed that drug aggregates can be forced to migrate to the surface of the fibers during electrospinning because of the semi-crystalline nature of PCL [33]. Another major reason for the release of DPA during the first stage is the rapid dissolution of PEG in the medium. There have been previous reports on fast erosion of PEG or similar polymers in polymeric blends that led to burst release phenomena and changes in the structure and diameter of the fibers [33,35]. Kim et al. also described the possibility of phase separation between the semi-crystalline PCL and the water soluble polyethylene oxide (PEO) that might have led to a core skeleton mainly composing of PCL and a surrounding coating of PEO [33]. The latter could cur during electrospinning, when the blend solution is quickly ejected to the collector, while fast solvent evaporation could enable phase separation between PCL and PEG. The use of a low molecular weight PEG for fibers F3 led to a faster release of DPA and to a more intense burst phenomenon during the first

**Table 2** Characteristic peaks ( $\text{cm}^{-1}$ ) in the FTIR spectra of the bulk materials (PCL, PEG and DPA) and in the FTIR spectra of F0 and F1 electrospun fibers.

Sample	Peaks ( $\text{cm}^{-1}$ )				
	-CH <sub>3</sub> , asymmetric stretching	-C=O, stretching	-C=N stretching	-CH <sub>3</sub> , scissoring and bending	-C-O-C-(ether), stretching
DPA bulk	2921		1531		
PCL bulk	2943	1725			
PEG 35k bulk	2882			1342	1095
F0	2946	1723		1342	1103
F1	2946	1726	1536	1342	1100

hours. The average molecular weight and thus the length of the polymeric chains affects the degradation rate of the polymer [8]. The release rate from F5 fibers was found to be the fastest, which is possibly due to the amorphous regions of PCL and the tendency of the molecules to travel near the surface of the fibers. Moreover, the absence of PEG might have resulted in lower homogeneity of the blend solution, leading to a more intense phase separation during electrospinning and consequently a higher percentage of DPA present on the surface of the fibers. F1 fibers were the most appropriate for sustained release of DPA exhibiting the lowest burst release suggesting that PEG could be beneficial in a polymeric blend rendering it suitable as a DDS. On the other hand, during the second stage, the release of DPA was slower and more gradual, mainly depending on diffusion. The cumulative release of the drug was mainly attributed to the diffusion of DPA through the polymeric matrix combined with the initial erosion of PEG (only for specimens F1 and F3). During the second stage of the release there is no PCL degradation [8], while the vast amount of PEG had been already dissolved into the medium. Therefore, the release of DPA from the electrospun fibers is predominantly controlled by Fickian diffusion, while the addition of PEG to the blend solution and its molecular weight did not affect the release.

## Conclusion

Blend electrospinning can be used to fabricate PCL/PEG fibers loaded with DPA, which can be used as a DDS. The addition of DPA to the polymeric blend used for electrospinning resulted in thinner, stronger and stiffer fibers. Moreover, the polymer chain length of the PEG can be used as a tool to adjust fiber properties if necessary. The electrospun fibers show sustained release of DPA, mainly through Fickian diffusion, indicating that they are suitable as drug delivery carriers, as long as the initial burst phenomenon is controlled.

## Acknowledgements

This research was granted by the German Research Foundation (Deutsche Forschungsgemeinschaft, DFG) by the Cluster of Excellence REBIRTH (From Regenerative Biology to Reconstructive Therapy, DFG EXC 62/1). The authors express their sincere gratitude to fellow researcher Poulami Basu MSc from the Biomedical Engineering Division (Vellore Institute of Technology, Vellore, India), for editing the manuscript, as well as Dipl.-Ing. Panagiotis Kalozoumis from the Department of Cardiothoracic, Transplantation and Vascular Surgery (Hannover Medical School, Hannover, Germany), for his contribution to the mechanical tensile tests that were performed.

## References

- 1 Szentivanyi AL, Zernetsch H, Menzel H, Glasmacher B (2011) A review of developments in electrospinning technology: New opportunities for the design of artificial tissue structures. *Int J Artif Organs* 34: 986-997.
- 2 Okutan N, Terzi P, Altay F (2014) Affecting parameters on electrospinning process and characterization of electrospun gelatin nanofibers. *Food Hydrocoll* 39: 19-26.
- 3 Sill TJ, von Recum HA (2008) Electrospinning: Applications in drug delivery and tissue engineering. *Biomaterials* 29: 1989-2006.
- 4 Szentivanyi A, Chakradeo T, Zernetsch H, Glasmacher B (2011) Electrospun cellular microenvironments: Understanding controlled release and scaffold structure. *Adv Drug Deliv Rev* 30: 209-220.
- 5 Zamani M, Prabhakaran MP, Ramakrishna S (2013) Advances in drug delivery via electrospun and electrosprayed nanomaterials. *Int J Nanomedicine* 8: 2997-3017.
- 6 Zernetsch H, Repanas A, Gryshkov A, Al Halabi F, Rittinghaus T, et al. (2013) Solving Biocompatibility Layer by Layer: Designing Scaffolds for Tissues. *Biomed Tech* 2013-4065.
- 7 Pfeiffer D, Stefanitsch C, Wankhammer K, Müller M, Dreyer L, et al. (2014) Endothelialization of electrospun polycaprolactone (PCL) small caliber vascular grafts spun from different polymer blends. *J Biomed Mater Res A* 102: 4500-4509.
- 8 Woodruff MA, Hutmacher DW (2010) The return of a forgotten polymer-Polycaprolactone in the 21st century. *Prog Polym Sci* 35: 1217-1256.
- 9 Repanas A, Zernetsch H, Glasmacher B (2014) Core/Shell electrospun fibers as biodegradable scaffolds for sustained drug delivery in Wound Healing applications. *Pneumologie*.
- 10 Repanas A, Zernetsch H, Mavrilas D, Glasmacher B (2014) Chitosan/Polycaprolactone electrospun biodegradable scaffolds for Cardiovascular Tissue Engineering. *Pneumologie*.
- 11 Zamani M, Morshed M, Varshosaz J, Jannesari M (2010) Controlled release of metronidazole benzoate from poly  $\epsilon$ -caprolactone electrospun nanofibers for periodontal diseases. *Eur J Pharm Biopharm* 75: 179-185.
- 12 Zhang YZ, Wang X, Feng Y, Li J, Lim CT, et al. (2006) Coaxial electrospinning of (fluorescein isothiocyanate-conjugated bovine serum albumin)-encapsulated poly( $\epsilon$ -caprolactone) nanofibers for sustained release. *Biomacromolecules* 7: 1049-1057.
- 13 Gaudio CD, Ercolani E, Galloni P, Santilli F, Baiguera S, et al. (2013) Aspirin-loaded electrospun poly( $\epsilon$ -caprolactone) tubular scaffolds: potential small-diameter vascular grafts for thrombosis prevention. *J Mater Sci Mater Med* 24: 523-532.
- 14 Radhakrishnan J, Krishnan UM, Sethuraman S (2014) Hydrogel based injectable scaffolds for cardiac tissue regeneration. *Biotechnol Adv* 32: 449-461.
- 15 Tungprapa S, Jangchud I, Supaphol P (2007) Release characteristics of four model drugs from drug-loaded electrospun cellulose acetate fiber mats. *Polymer* 48: 5030-5041.
- 16 Miyajima M, Koshika A, Okada J, Kusai A, Ikeda M (1998) Factors influencing the diffusion-controlled release of papaverine from poly (L-lactic acid) matrix. *J Control Release* 56: 85-94.
- 17 Fong H, Chun I, Reneker DH (1999) Beaded nanofibers formed during electrospinning. *Polymer* 40: 4585-4592.
- 18 Lam CXF, Savalani MM, Teoh SH, Hutmacher DW (2008) Dynamics of in vitro polymer degradation of polycaprolactone-based scaffolds: accelerated versus simulated physiological conditions. *Biomed Mater*.
- 19 Sacco RL, Diener HC, Yusuf S, Cotton D, Ounpuu S, et al. (2008) Aspirin and extended-release dipyridamole versus clopidogrel for recurrent stroke. *N Engl J Med* 359: 1238-1251.
- 20 Zhuplatov SB, Masaki T, Blumenthal DK, Cheung AK (2006) Mechanism of dipyridamole's action in inhibition of venous and arterial smooth muscle cell proliferation. *Basic Clin Pharmacol Toxicol* 99: 431-439.
- 21 Begandt D, Bader A, Gerhard L, Lindner J, Dreyer L, et al. (2013) Dipyridamole-related enhancement of gap junction coupling in the GM-7373 aortic endothelial cells correlates with an increase in the amount of connexin 43 mRNA and protein as well as gap junction plaques. *J Bioenerg Biomembr* 45: 409-419.
- 22 Begandt D, Bader A, Dreyer L, Eisert N, Reeck T, et al. (2013) Biphasic increase of gap junction coupling induced by dipyridamole in the rat aortic A-10 vascular smooth muscle cell line. *J Cell Commun Signal* 7: 151-160.
- 23 Punnakitikashem P, Truong D, Menon JU, Nguyen KT, Hong Y (2014) Electrospun biodegradable elastic polyurethane scaffolds with dipyridamole release for small diameter vascular grafts. *Acta Biomater* 10: 4618-4628.
- 24 Repanas A, Glasmacher B (2015) Dipyridamole embedded in Polycaprolactone fibers prepared by coaxial electrospinning as a novel drug delivery system. *J Drug Deliv Sci Technol* 29: 132-142.
- 25 Ritger PL, Peppas NA (1987) A simple equation for description of solute release II. Fickian and anomalous release from swellable devices. *J Controlled Release* 5: 37-42.
- 26 Yu H, Jia Y, Yao C, Lu Y (2014) PCL/PEG core/sheath fibers with controlled drug release rate fabricated on the basis of a novel combined technique. *Int J Pharm* 469: 17-22.
- 27 Maleki M, Amani-Tehran M, Latifi M, Mathur S (2014) Drug release profile in core-shell nanofibrous structures: A study on Peppas equation and artificial neural network modeling. *Comput Methods Programs Biomed* 113: 92-100.
- 28 Saraf A, Lozier G, Haesslein A, Kasper FK, Raphael RM, et al. (2009) Fabrication of Nonwoven Coaxial Fiber Meshes by Electrospinning. *Tissue Eng Part C Methods* 15: 333-344.
- 29 Lee CK, Kim SI, Kim SJ (2005) The influence of added ionic salt on nanofiber uniformity for electrospinning of electrolyte polymer. *Synth Met* 154: 209-212.
- 30 Cramariuc B, Cramariuc R, Scarlet R, Manea LR, Lupu IG, et al. (2013) Fiber diameter in electrospinning process. *J Electrostat* 71: 189-198.
- 31 Natu MV, De Sousa HC, Gil MH (2013) Influence of polymer processing technique on long term degradation of poly( $\epsilon$ -caprolactone) constructs. *Polym Degrad Stab* 98: 44-51.
- 32 Gautam S, Dinda AK, Mishra NC (2013) Fabrication and characterization of PCL/gelatin composite nanofibrous scaffold for tissue engineering applications by electrospinning method. *Mater Sci Eng C* 33:1228-1235.
- 33 Kim TG, Lee DS, Park TG (2007) Controlled protein release from electrospun biodegradable fiber mesh composed of poly( $\epsilon$ -caprolactone) and poly(ethylene oxide). *Int J Pharm* 338: 276-283.
- 34 Stylianopoulos T, Bashur CA, Goldstein AS, Guelcher SA, Barocas VH (2008) Computational predictions of the tensile properties

- of electrospun fibre meshes: Effect of fibre diameter and fibre orientation. *J Mech Behav Biomed Mater* 1: 326-335.
- 35 Saraf A, Baggett LS, Raphael RM, Kasper FK, Mikos AG (2010) Regulated non-viral gene delivery from coaxial electrospun fiber mesh scaffolds. *J Controlled Release* 143: 95-103.
- 36 Valarezo E, Tammaro L, González S, Malagón O, Vittoria V (2013) Fabrication and sustained release properties of poly( $\epsilon$ -caprolactone) electrospun fibers loaded with layered double hydroxide nanoparticles intercalated with amoxicillin. *Appl Clay Sci* 72: 104-109.
- 37 Jannesari M, Varshosaz J, Morshed M, Zamani M (2011) Composite poly(vinyl alcohol)/poly(vinyl acetate) electrospun nanofibrous mats as a novel wound dressing matrix for controlled release of drugs. *Int J Nanomedicine* 6: 993-1003.
- 38 Song B, Wu C, Chang J (2012) Dual drug release from electrospun poly(lactic-co-glycolic acid)/mesoporous silica nanoparticles composite mats with distinct release profiles. *Acta Biomater* 8: 1901-1907.